Report
P-17-12
February 2017

Study of high-frequency seismic signals in the Forsmark area

Björn Lund
Reynir Bödvarsson
Lars Dynesius
Michael Schieschke

SVENSK KÄRNBRÄNSLEHANTERING AB

SWEDISH NUCLEAR FUEL
AND WASTE MANAGEMENT CO

Box 3091, SE-169 03 Solna
Phone +46 8 459 84 00
skb.se

SVENSK KÄRNBRÄNSLEHANTERING

ISSN 1651-4416
SKB P-17-12
ID 1478243

February 2017

Study of high-frequency seismic signals in the Forsmark area

Björn Lund, Reynir Bödvarsson,
Lars Dynesius, Michael Schieschke
Department of Earth Sciences, Uppsala University

Summary

The proposed nuclear waste repository in Forsmark will be equipped with a high resolution seismic monitoring network. The network will monitor natural seismicity as well as seismic events induced by the construction, operation and closure of the repository and the subsequent evolution of the repository.

In order to determine which type of seismic sensors will give optimum performance in the repository area, and how these should be spaced, it is necessary to know the level and frequency content of the seismic background signals. The objective of this report is to study high-frequency seismic signals in the Forsmark area and the effect of seismic noise generated by the Forsmark power plants.

Three borehole sensors were bought from the Institute of Mine Seismology (IMS) in South Africa which contain both a five-element geophone assembly and an accelerometer. The sensors were connected to data loggers rented from IMS, with 24-bit digitizers, GPS-timing and data storage on USB-sticks. During the activity the instrumentation was both thoroughly tested in the laboratory at the Swedish National Seismic Network (SNSN), Uppsala University, and used in temporary installations in boreholes at six locations in Forsmark.

One of the main results of this study is the realization that with geophones with too low sensitivity (corresponding to normal single geophone sensitivity, 80 V/m/s), it is not possible to record true ground motion in the frequency band of interest for the repository seismic network. We found that geophones with nominal sensititvity of at least 400 V/m/s, given the noise characteristics of the IMS digitizer, should be used to be able to record true ground motion over the entire repository area. An additional, external high-quality pre-amlifier would also increase the sensitivity. Borehole geophones should be used, and once these are thoroughly coupled to the bedrock, e.g. by cementing, the response will most likely improve in certain frequency bands over what we have seen in this study. Geophones typically perform well up to frequencies of approximately 2 kHz. For higher frequencies accelerometers would be necessary.

There is significant seismic noise from the nuclear power plants in the repository region, both wide-band noise below 100 Hz and narrow-band high-noise levels at higher frequencies. This will be a challenge for the repository seismic network. We suggest that the network initially is instrumented with a limited number of high-sensitivity geophones, ideally placed in boreholes at 30–200 m depth, below the gently dipping fracture zone that covers much of the repository area. The borehole stations should be augmented by a few surface stations, especially in the vicinity of the construction of the tunnel. As excavations progress and seismic events from the construction are being analyzed, the network should be gradually expanded based on the need to improve the analysis and to cover certain volumes more accurately. If smaller seismically active volumes are identified at depth, then there may be a need for a dense installation of geophones or accelerometers in that volume. The repository network should also be linked to the Swedish National Seismic Network (SNSN) in order to improve the analysis of larger events.

The type of instrumentation needed for the repository network depends not only on the seismic background environment but also on factors such as the desired detection level, station density and rock type. We suggest that this activity is followed by a seismic network design phase where all factors are taken into account and an initial network geometry is proposed. We also suggest that the initial network be regarded as the first step, and that subsequent studies of events during tunneling form a basis for expansion of the network.

Sammanfattning

Det föreslagna kärnbränsleförvaret i Forsmark kommer att utrustas med ett känsligt seismiskt övervakningssystem. Systemet kommer att detektera både naturlig seismicitet men också seismiska händelser som induceras under byggandet, driften och stängningen av förvaret samt under förvarets framtida utveckling.

För att bestämma vilken typ av seismiska sensorer som fungerar bäst i miljön runt förvaret, samt hur dessa ska fördelas i området, behövs kunskap om nivåer och frekvensinnehåll i den nu förekommande seismiska bakgrundsmiljön. Syftet med denna rapport är att studera de högfrekventa seismiska bakgrundssignalerna i Forsmarksområdet och effekten av det bakgrundsbrus som genereras av kärnkraftsverken i Forsmark.

Tre borrhålssensorer köptes in från Institute of Mine Seismology (IMS) i Sydafrika. Dessa innehåller både en fem-elements geofon och en accelerometer. Sensorerna kopplades till datainsamlingssystem som hyrdes in från IMS, dessa hade 24-bitars A/D-omvandlare, GPS-tidsstyrning samt datalagring på USB-stickor. Under denna studie testades instrumenteringen noggrannt i laboratoriet hos det svenska nationella seismiska nätet (SNSN) innan den användes i tillfälliga installationer i grunda borrhål på sex olika platser i förvarsområdet i Forsmark.

Ett av huvudresultatet i studien är att med gefoner med för låg känslighet, motsvarande normal känslighet hos geofoner med endast ett element (80 V/m/s), är det inte möjligt att mäta upp bakgrundssignalernas markrörelser i det frekvensband som är av intresse för förvarets seismiska nätverk. Studien visar att geofoner med en nominell känslighet av minst 400 V/m/s, givet bruskaraktäristiken på IMS datainsamlingssystem, bör användas för att kunna registrera korrekt markrörelse över hela förvarsområdet. Systemets känslighet kan även förstärkas med en extern förstärkare mellan geofon och datainsamlingsenhet. Borrhålsgeofoner bör användas och det är troligt att de, när de gjutits fast i berget, kommer att leverera något bättre karaktäristik i vissa frekvensband än de vi ser i denna studie. Geofoner klarar som regel av att på ett korrekt sätt samla in data upp till cirka 2 kHz. För högre frekvenser krävs accelerometrar.

Kärnkraftverken i förvarets närhet genererar signifikant seismiskt brus, både bredbandigt brus under 100 Hz och smalbandigt brus vid högre frekvenser. Detta brus blir utmanande för det seismiska systemet att hantera. Vi föreslår i studien att förvarsnätverket först instrumenteras med ett mindre antal högkänsliga borrhålsgeofoner, i borrhål mellan 30–200 m djup nedanför den flacka sprickzon som går igenom mycket av förvaret. Borrhålsstationerna bör kompletteras med ett par stationer på markytan i närheten av konstruktionen av tunneln. Allteftersom arbetet framskrider och tunneln fördjupas bör nätverket gradvis expanderas baserat på behovet av att förbättra den seismiska analysen samt att övervaka en större bergvolym. Om mindre, seismiskt aktiva bergvolymer identifieras under konstruktionsarbetet kan det finnas behov av att installera flera geofoner eller accelerometrar i de specifika områdena. Förvarets seismiska system bör också kopplas till SNSNs nätverk för att förbättra analysen av större seismiska händelser.

Vilken typ av instrument som krävs för kärnbränsleförvarets seismiska nätverk beror inte enbart på den seismiska bakgrundsmiljön utan också på faktorer som önskad detektionsnivå, stationstäthet och typen av berg. Vi föreslår att denna studie följs av en designfas för ett seismiskt nätverk där alla faktorer tas hänsyn till och som föreslår en preliminär nätverksgeometri. Vi understryker också att detta är det första steget, som bör följas av steg där analysen av den seismiska aktiviteten i tunneln ligger till grund för expansion av nätverket.

Contents

1 Introduction

The proposed nuclear waste repository in Forsmark will be equipped with a high resolution seismic monitoring network. The network will monitor natural seismicity as well as seismic events induced by the construction, operation and closure of the repository and the subsequent development of the repository. In order to determine which type of seismic sensors will give optimum performance in the repository area, and how these should be spaced, it is necessary to know the level and frequency content of the seismic background signals. The objective of this report is to study high-frequency seismic signals in the Forsmark area and the effect of noise levels generated by the Forsmark power plants. Previously, lower frequency (up to 500 Hz) seismic and electromagnetic background signals have been studied (Lund et al. 2012) and significant seismic noise was identified in the vicinity of the Forsmark nuclear power plants. The activity reported here has three objectives: (i) Investigate the seismic background signals in the Forsmark area at higher frequencies, up to about 10 kHz. (ii) Study which sensitivity the instrumentation would need in order to operate well in the noisy environment at Forsmark. (iii) Test how well custom made sensors from the Institute for Mine Seismology (IMS) perform in the Forsmark environment.

During June 2013, 60 cm deep boreholes were drilled for the seismic sensors. The measurements were planned for August/September 2013, but due to significant delays in the delivery of the instruments the measurements could not be performed until October/November 2013. Measurements were made with three sensors simultaneously at two locations, followed by a deployment of sensors in a NW-SE profile across the proposed repository area.

2 Instrumentation used

For this activity, SKB purchased three identical sets of sensors from the Institute of Mine Seismology (IMS, http://www.imseismology.org) in South Africa. IMS is one of the leading manufacturers of mine seismology instrumentation and also provides analysis of, and analysis tools for, mine seismicity. In Sweden, IMS has installations in Kiruna, Malmberget and Zinkgruvan. For the testing period in this activity, SKB also rented three data loggers with 24-bit digitizers from IMS that were used for field and lab measurements.

The sensors consisted of five geophone elements connected in series and an accelerometer, all of which were enclosed in a 34 mm diameter steel casing of approximately 30 cm length, see Figure 2-1. The sensor combination measures vertical motion only. Some of the characteristics of the sensors are listed in Table 2-1 (see Appendix A for a full set) and Figure 2-2.

After initial field tests we manufactured 2 kg lead weights that were attached to the top of the sensor assemblies in order to stabilize them in the boreholes and increase the coupling to the ground, see discussion in Chapter 4 and photo in Figure 2-1

Table 2-1. Sensor specifications.

Sensor	Geophone element	Accelerometer element, 25 kHz
Natural frequency	14 Hz ± 7 %	
Configuration	Uniaxial, vertical	Uniaxial, vertical
Open circuit sensitivity	80 V/m/s +5 /−10 %	100 mV/g ± 5 %
Coil resistance	3500 Ω	
Open circuit damping	0.185	
Broadband noise		150 μg
	Geophone assembly	
Coil resistance	17500 Ω	
Open circuit sensitivity	400 V/m/s	
Nominal damping resistor	41 kΩ	

Figure 2-1. *Photos of the data logger, external connection boxes and cables (left) and the sensor assembly with the added 2 kg lead weight (right).*

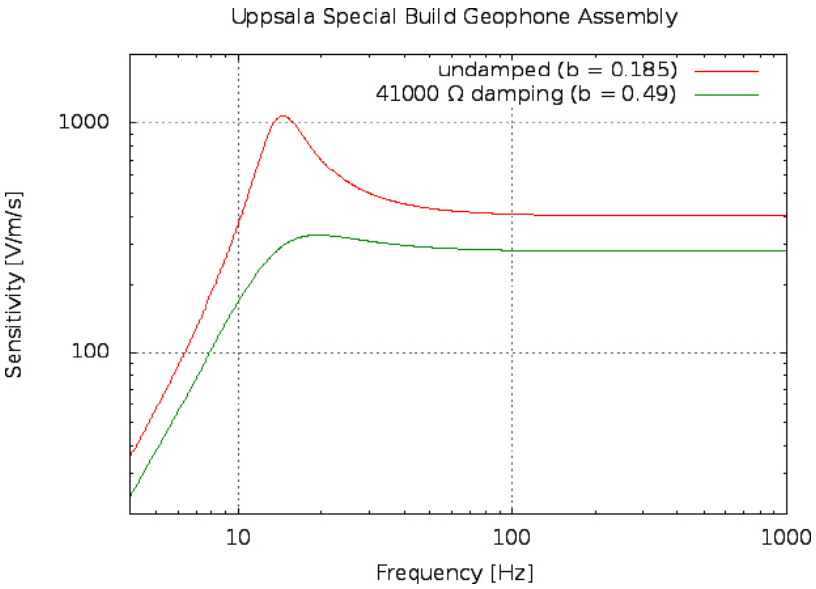

Figure 2-2. *Frequency response of the geophone assembly as supplied by IMS.*

2.1 Problems encountered with the instrumentation

There were significant delays in the delivery of the equipment from IMS to Uppsala University. The equipment was ordered from IMS on 2013-04-19 with delivery set to 4–6 weeks. After significant delays, the shipment arrived in Sweden in late September, and was then held in customs until the first week of October.

Setting up the instruments proved rather difficult, as there was very little documentation and all questions had to go via email to IMS. The IMS support did, however, respond well. Below is a list of some of the major problems:

- Not enough information on how to install the software Neuron, used for data logger configuration.
- License problems, the USB-dongle with the Neuron license could not be made to work, instead we eventually received a machine specific license.
- Manual replacement of configuration files in Neuron was necessary for the software to recognize the data logger.
- Neuron requires more powerful computers than our field computers, which meant that all configuration had to be done in the lab, and could not be done in the field.
- Unexpectedly, the data logger required a continuous GPS-signal in order to operate in “stand-alone” mode. Without “stand-alone” mode we could not communicate with the data logger, and it could therefore not be configured indoors. This was solved by physically disassembling the GPS antenna from the logger unit, and placing it outdoors.
- Two out of three loggers were wired erroneously which meant that they did not work. The problem was identified by our engineers, IMS sent a new wiring scheme and we manufactured new cables.
- No documentation of a rather complicated way of enabling continuous measurements through well hidden menus. When continuous mode was finally activated, it still did not work as it had been disabled in the firmware. IMS sent a new firmware version.
- We identified a firmware bug which caused data loss during continuous measurements. Manual addition of configuration files solved the problem.
- The built-in web server, part of the firmware, did not work. IMS sent a new firmware version.

2.2 Instrument response

We converted the waveform data from an internal IMS format to SAC format in a two stage process using first MATLAB code provided by IMS to get the data into MATLAB and then wsac.m, a MATLAB script in Michael Thorne's SACLAB (SACLAB 2014), to write binary SAC files. In the first versions of the IMS data conversion software the instrument response was removed from the data internally so the data was provided in m/s or m/s^2 for the geophones and accelerometers, respectively. Tests of the instruments revealed, however, that the initial set of instrument responses were incorrect and in later versions of the software the data could be provided without instrument deconvolution. Problems included a polarity error in the geophone data, faulty geophone response and accelerometer data given in "g" instead of m/s^2. The final set of responses are given below. Note that we (and IMS) ignore the small hump in the instrument response at frequencies just above the natural frequency, see Figure 2-2, for the geophones and only use a scale factor.

Digitizer: the digitizer is 24-bit with 0–5.65 V input and an internal scale factor of 16 (due to "The first four bits of data stored to disk are status flags and not related to the ADC conversion result. We divide by 16 to remove these bits." (D. Bredenkamp, personal communication, 2013-11-22).

The conversion from counts to Volt is therefore:

$Volt = counts \times (5.65/(2^{24} - 1)) \times (1/16) = counts \times 2.104789e{-}8$

Geophones: Sensitivity 400 V/m/s, coil resistance 17.5 kΩ, damping resistor 41 kΩ, internal digitizer resistance 100 kΩ. This gives:

total_damping = geophon_damp × digitizer_damp/(geophon_damp + digitizer_damp) = 29 078 Ω

damped_sensitivity = sensitivity × total_damping/(total_damping + coil_resistance) = 249.7 V/m/s

This gives a total geophone conversion factor of:

m/s = 8.428784e–11 × counts (11.865 cnt/nm/s)

We see that the five serially connected geophones give a damped sensitivity of 250 V/m/s compared to the standard IMS 14 Hz single geophone damped sensitivity of 60 V/m/s (Appendix B). We therefore gain a factor 4.2 in the response.

Accelerometers: Sensitivity 0.1V/g = 0.010194 $V/m/s^2$

$m/s^2 = 2.064798e{-}06 \times counts$

In our field test with a Guralp instrument, see Section 2.4 below, we used a Guralp Compact seismometer, T34357, and a Guralp digitizer and data logger A752. The Z-component of the sensor has sensitivity 9 806 V/m/s in the flat part of the spectrum, i.e. from about 50 seconds to approximately 85 Hz. The digitizer response is 3.211 µV/cnt for the Z-component. The total conversion factor is thus:

m/s = 3.274526e–10 × counts (3.054 cnt/nm/s).

2.3 Laboratory tests of the instrumentation

In our laboratory we tested the performance of the digitizer and data logger. We were specifically interested in the internal noise level and noise characteristics of the digitizer, and the time syncronization to the GPS. In the discussion and figures below we have referenced the digitizer output to ground motion as would have been measured with an attached geophone or accelerometer. We performed the following two tests:

2.3.1 Digitizer noise

Using three channels, we substituted the sensors with appropriate resistors in order to evaluate the internal noise of the digitizer. On channel 1, the accelerometer was substituted with a 1 kΩ resistor, on channel 2 the geophone assembly was substituted by a 12.2 kΩ resistor and on channel 3 we connected a 50 Ω resistor as a comparison of less current noise with respect to the other two channels. Measurements were done at both 6 kHz and 24 kHz, with and without the ethernet running, and with and without a connection to the lab grounding point.

In Figure 2-3 we show the results of tests at 6 kHz sampling frequency and a simulated geophone assembly (blue) and the 50 Ω resistor (red). We see that the noise levels are generally low, at 6–7 nm/s at 1 Hz, reducing to approximately 3–4 nm/s at higher frequency. The noise floor is relatively flat from 50 Hz up. This is in agreement with measurements performed at the IMS lab in response to our inquiries, where they estimated an electronic noise RMS of 1.144 µV, corresponding to 4.1 nm/s (D. Bredenkamp, IMS, personal communication 2013-11-22). We also note, as expected, that with the 12.2 kΩ resistor the resistor wiring acts like an antenna and picks up the 50 Hz and overtones elektromagnetic signals from the grid. The average noise levels are very similar between the two recordings, the 50 Ω resistor showing slightly lower noise.

Our tests also showed slightly higher noise levels when the data logger was attached to the lab grounding point (on the building's grid). We also noted a very distinct noise peak at 480 Hz when the data logger internal ethernet communication was turned on, see Figure 4-4. This has also been confirmed by IMS (D. Bredenkamp, IMS, personal communication 2013-11-15).

Figure 2-4 shows the results of the tests with a 1kΩ resistor simulating the accelerometer. As seen in the Figure, the accelerometer simulation is very noisy. This is likely due to a noisy preamplifier, which is external to the data logger (see grey round plastic boxes on the photo in Figure 2-1). The longer period noise could be explained by noise increasing as the inverse of frequency, which is commonly observed in amplifiers.

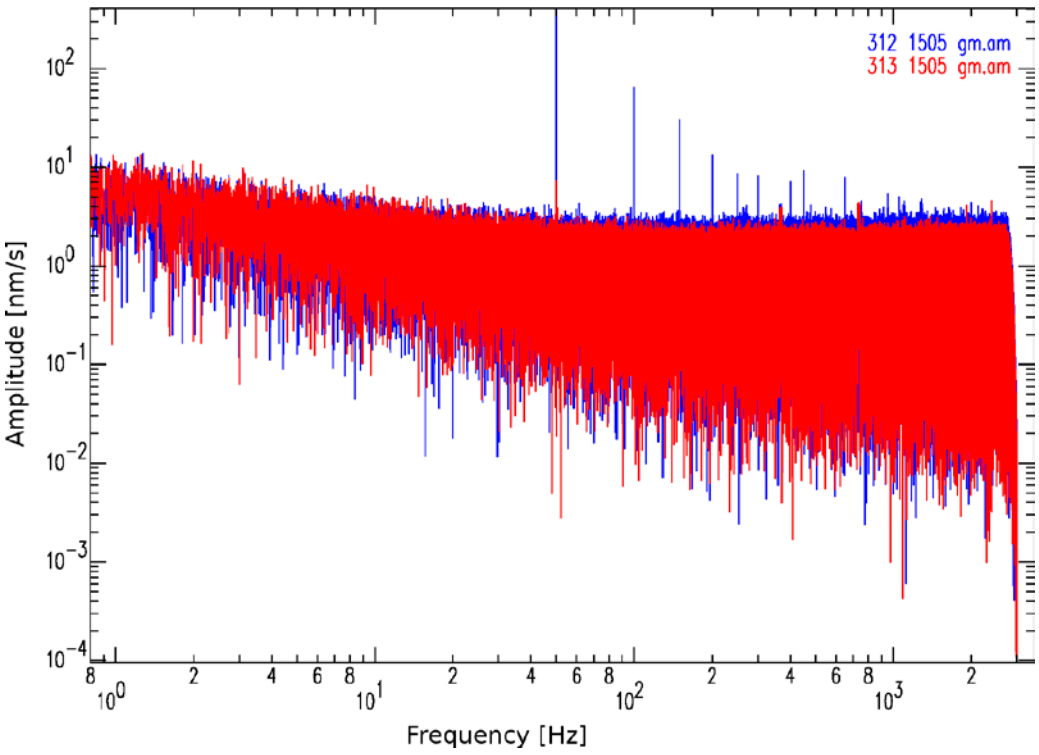

Figure 2-3. *Digitizer and data logger internal noise spectra from 0.8 Hz to 3 kHz. Amplitude as simulated ground motion, nm/s. 12.2 kΩ resistor (blue), 50 Ω resistor (red).*

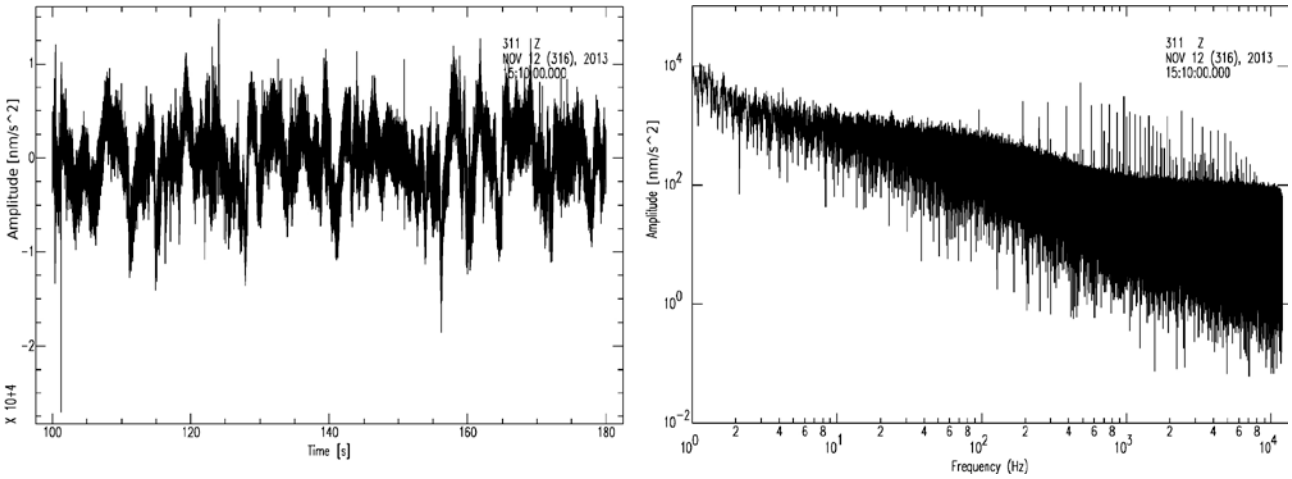

Figure 2-4. *Preamplifier, digitizer and data logger noise. Amplitude in ground acceleration (nm/s^2) as simulated for an accelerometer with a 1 kΩ resistor. Left: Time series, right: spectrum.*

2.3.2 Time syncronization

We connected a high precision GPS controlled reference clock with 1 sec pulses to the data logger's analogue input in order to test the time keeping. The sample frequency was set to 24 kHz. Figure 2-5A shows a short time series of the second-pulses sent by the reference clock and Figure 2-5B shows the rising and falling edge offset over time. We see that the time drift in the logger is accumulating to 1 ms in 5 minute intervals and then adjusted. This is done exclusively in the post-processing software which IMS provided for this particular experiment. As seen in Figure 2-5B, the sampling clock frequency is slightly lower than 24 kHz during our test. The post processing software compensates for the drift by adding the number of missing samples, with a value of zero. The effect of this is negligible in our analysis here. However, in a continuously recording system the procedure produces a non-acceptable error. IMS has informed us that they handle the timing more accurately in their networked production systems, which normally operates with triggered short segmented data. For continuously recording systems the internal clock should be phase-locked to the GPS, a feature not yet implemented in the IMS system.

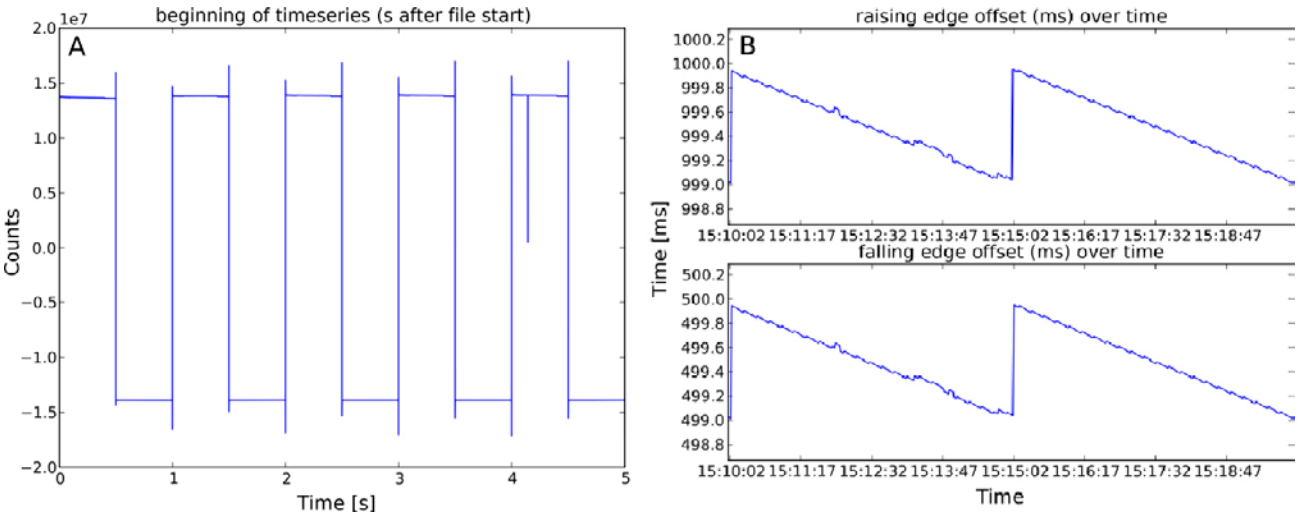

Figure 2-5. *Test of logger timing accuracy using an external high resolution GPS clock. A) Time series of second pulses from the reference clock. B) The rising (upper) and falling (lower) edges in milliseconds versus time.*

2.4 Field tests of the instrumentation

The sensor response information and processing of the data was tested in the field at Forsmark, using all three sensors in three boreholes located close (10 cm distance) to each other, attached to the same data logger, at site 6 (see map in Figure 3-1). We performed the following three tests:

2.4.1 Hammer blows

In Figure 2-6 we show the recordings of a hammer blow 5 m away from the sensor array. The instrument response has been removed from both geophone and accelerometer signal and the geophone signal has been differentiated to show acceleration. We see that the accelerometer signal is generally noisier than the geophone signal, but that the polarities of the two signals are the same, and that the amplitudes are very similar, at least in the early part of the wave train. In the first round of tests the polarities of the signals were opposite, which was due to a data conversion error for the geophone data.

2.4.2 Comparison to a broadband Guralp sensor

We made an overnight recording of the background noise, recording both with the IMS instruments and a Guralp Compact CMG-3ESPC broadband seismometer (60s-100Hz S/N T34357) attached to a Guralp DM-24-S3 (S/N A752) 24-bit digitizer and data logger, sampling at 500 Hz. The Guralp sensor was located 3 m from the sensor array, on top of the outcrop. The comparison of the sensors is shown in Figure 2-7. The geophone signal was sampled at 6 kHz but decimated to 500 Hz to compare to the Guralp signal. We see that the two instruments show very similar amplitudes from 13–14 Hz up to approximately 60 Hz. Below 13 Hz the geophone sensitivity diminishes rapidly and the instrument does not capture the full amplitude of the wide noise peak between 4 and 14 Hz. For the same reason it does not capture the high amplitude microseisms below 1Hz. Above 60 Hz, the IMS geophone shows lower noise levels than the Guralp instrument. The Guralp may be affected by a noisier digitizer. The increase in amplitude in the IMS geophone at 150 Hz will be discussed further below. Zooming in on the strong 50 Hz signal, to the right in Figure 2-7, we see that there is some unresolved difference in the amplitudes recorded by the Guralp and the IMS geophone, but that they are generally very similar. The IMS system produces slightly higher amplitudes than the Guralp system. These differences could be due to differences in the coupling to the bedrock.

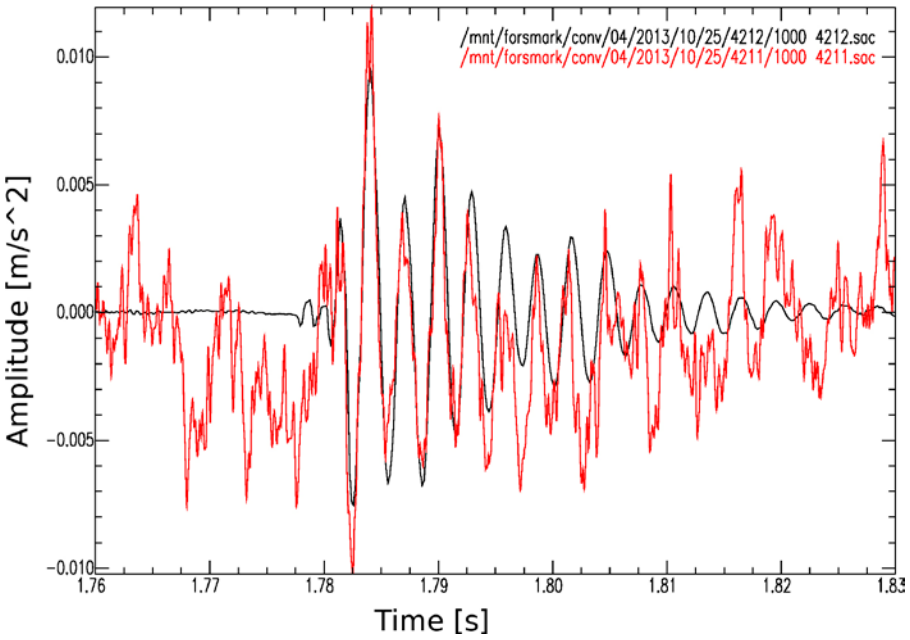

Figure 2-6. *A hammer blow recorded at 5 m distance by one of the combined geophone (black) and accelerometer (red) instrument.*

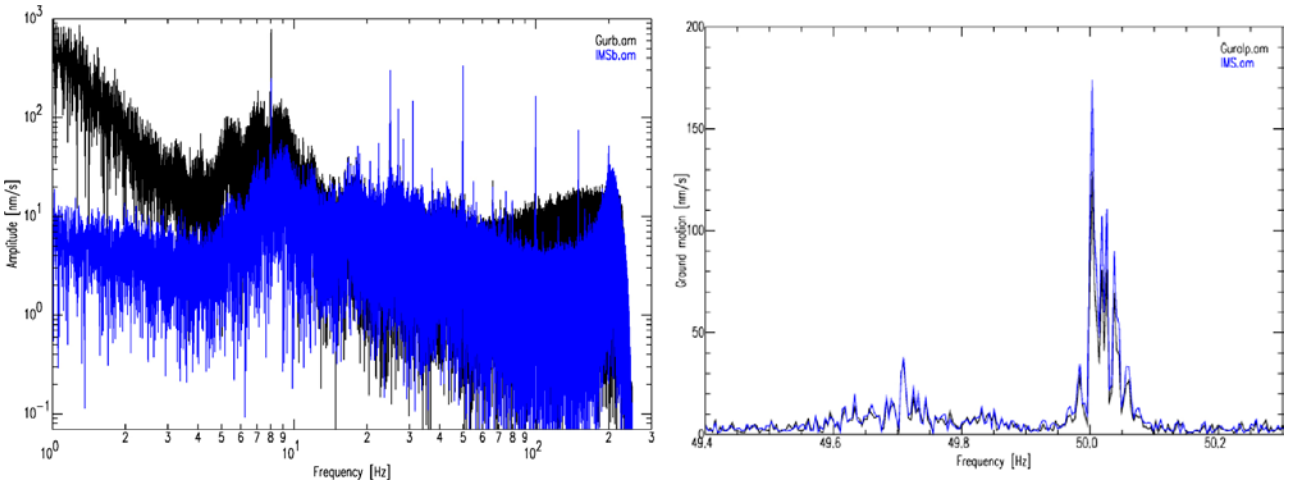

Figure 2-7. *Spectra of background seismic signals at site 6 in Forsmark, 10 minutes of data at 00:30 GMT on 28/11-2013. Vertical component of Guralp Compact (black) and IMS geophone (blue). Amplitude in ground motion [nm/s]. Left: Frequency content from 1 Hz to 250 Hz, logarithmic axes. Right: Zoom in around 50 Hz (49.4–50.4 Hz) with linear plot axes.*

2.4.3 Recording of a mine blast from the Dannemora mine, approximately 30 km away.

Our sensors captured blasts from the Dannemora mine during the field deployments. Figure 2-8 shows comparisons between the Guralp and IMS sensors for one of these blasts. We see that the amplitudes are generally the same, but the zoom in of the first part of the arriving wave shows that there is a shift in the arrival time on the two instruments, on the order of 0.01 s. This difference is not explained by the distance between the sensors, but may be related to the aforementioned timing problem with the IMS digitizer. The accelerometers did not record the Dannemora event above the noise level, it could not be seen in the accelerometer time series.

All in all, our field tests indicate that the instrument response information of the IMS system is sufficiently well known and that the system produces data which corresponds to that from one of our Guralp systems. We also conclude that the accelerometer systems are significantly noisier than the geophone systems.

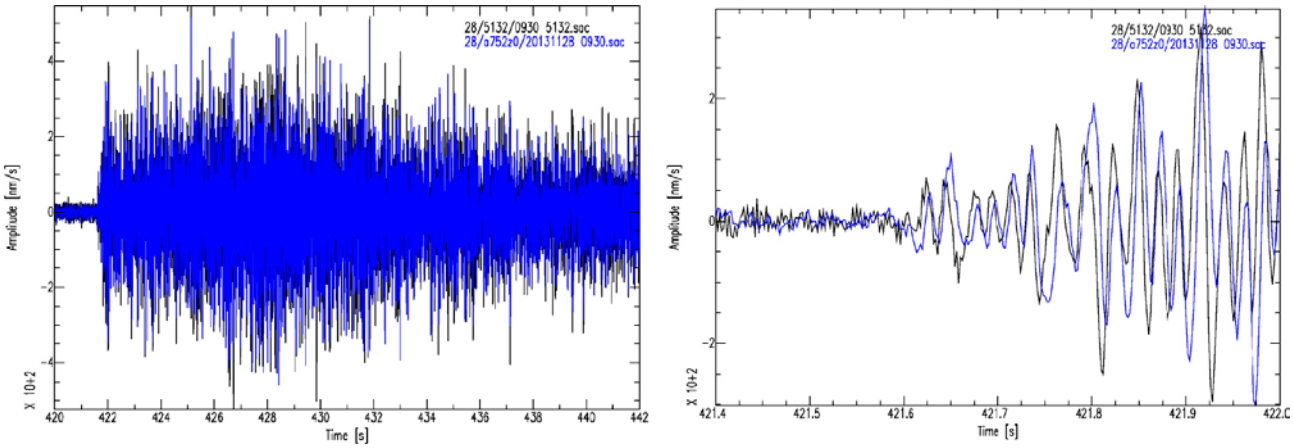

Figure 2-8. *Recording at site 6 of a blast in the Dannemora mine at 09:37 GMT on 28/11-2013, approximately 30 km away from the site. Guralp Compact recording (black) and IMS geophone recording (blue), amplitudes in true ground motion [nm/s], note the scale factor of 100 on the y-axes.*

3 Field measurements in Forsmark

We carried out nine sets of field measurements in the Forsmark area between 2013-10-22 and 2013-11-28, seven of these included continuous recording over night. The field campaign area is shown on the map in Figure 3-1, with the six sites where we sampled the seismic background field along an approximately northwest-southeast profile, see Table 3-1. At the sites, boreholes were drilled in good quality bedrock to 60 cm depth for the sensor installations. At sites 1 and 6, three boreholes were drilled to allow simultaneous recording with all three sensors for instrument testing purposes. The sensors were lowered into the boreholes until they rested firmly at the bottom. During drilling, the bottom of the boreholes were made as planar as possible, the state of the boreholes inspected by camera. In order to centralize the sensors in the boreholes we tested various approaches to sleeves around the upper part of the sensor, see e.g. Figure 2-1. We also water proofed the boreholes using special lids with holes through for the cable and sealing around the hole.

Table 3-1. Location (RT90 coordinates), distance to the nearest nuclear power plant and SKB Sicada ID for the six measurement locations.

Site	Easting	Northing	Distance to the nearest power plant [km]	Sicada ID
1	1630805	6701129		PFM007742
			0.41	PFM007743
				PFM007744
2	1631038	6700390	0.46	PFM007745
3	1631600	6700218	1.04	PFM007746
4	1632346	6699713	1.93	PFM007747
5	1633299	6698751	3.25	PFM007748
6	1633902	6698106	4.12	PFM007749
				PFM007750
				PFM007751

Figure 3-1. *Map of the Forsmark area with the six measurement sites. Site 1 is very close to the nuclear power plants Forsmark 1 and 2. Site 6 is the most distant site from the power plants.*

The first three sets of measurements indicated that the coupling between the sensor assembly and the bedrock was far from ideal. We tried to increase the coupling by adding a 2 kg lead weight onto the top of the sensor assembly. This did improve the recordings but it is likely that we still have significant noise in some frequency bands due to vibrations between the borehole and the sensor, see further below.

The following field measurements provided the data that is used in the analysis in this report:

1. Site 1, three sensors recording simultaneously, 2013-10-24–2013-10-25.
2. Site 6, three sensors recording simultaneously, 2013-11-06–2013-11-07.
3. Sites 1, 4 and 6, 2013-11-07–2013-11-08.
4. Sites 1, 2 and 3, 2013-11-13–2013-11-14.
5. Sites 4, 5 and 6, 2013-11-14–2013-11-15.
6. Site 6, simultaneous recording with one IMS and one Guralp Compact instrument, 2013-11-27–2013-11-28.

All recordings with the IMS sensors were done at 24 kHz sampling frequency. The geophone data was decimated to 6 kHz sampling in post-processing, as the geophones are specified up to 2 kHz. In Figure 3-3 we show a representative example of a simultaneous recording with all three sensor assemblies, i.e. three geophones and three accelermometers, from the quiet site 6. The Figure shows how the geophone signals are very similar, both in shape and amplitude, while the accelerometer signals vary significantly. In fact, the lowermost accelerometer may be faulty and should be returned to IMS for maintenance. We note that this type of accelerometer is designed to record high frequency accelerations near an event, and therefore does not have very high sensitivity. IMS confirmed (D. Bredenkamp, personal communication, 2014-02-12) that 0.01 m/s^2 peak noise is normal for these sensors. Although we observe peaks in the accelerometer spectra at frequencies above 2–3 kHz, it is unclear to us if these are natural events of just noise from the recording system. We suspect the latter based on the lab tests of the accelerometer input. In the following analysis we will focus on the more sensitive geophone data, as we are investigating mostly very weak signals that are not picked up by the accelerometers.

Figure 3-2. *Photographs of sensor deployment at site 6.*

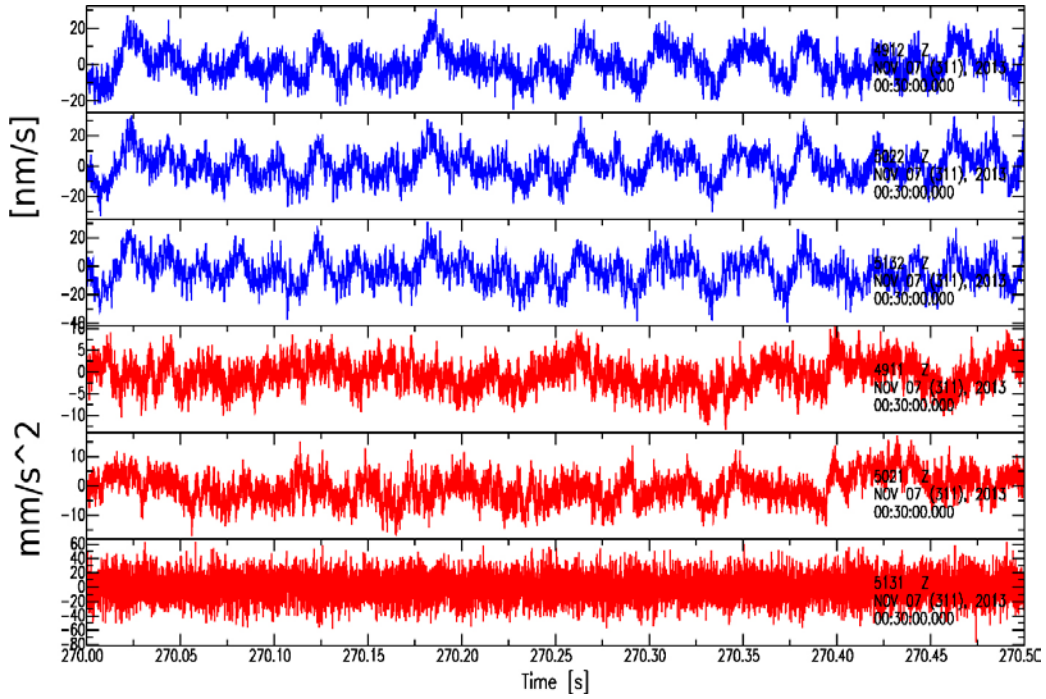

Figure 3-3. *Half a second time series from the geophones (blue) and accelerometers (red) recording simultaneously at site 6, on 2013-11-07 at 00:30 GMT.*

4 Frequency content of the signals

During three different time periods, the sensors were placed along the measurement profile in three different configurations. In Figures 4-1 to 4-3 below we show spectra from these three different recording periods, in order to display both the frequency dependence of the recorded signals at individual sites, and the variation in amplitude and frequency content along the profile.

We note some very characteristic features of the spectra in Figures 4-1 to 4-3. First, the wide spectral hump between approximately 4 and 200 Hz. This peak declines significantly with distance away from the nuclear power plants, indicating that it originates from the power generation and the associated infrastructure. Second, we see very clear, narrow-band peaks in the spectra, most prominent in the 50 Hz and overtone peaks. There are peaks all the way up until the highest attainable (Nyquist) frequency, and they are clearly visible at all distances. Third, we note a flattening of the spectra at approximately 200–300 Hz. Comparing the amplitude of the flat parts of the spectra to the laboratory tests on the digitizer in Figure 2-3, we find that the flat spectral section observed in the field measurements indicate that the background ground motion levels are below the internal electronic noise in the digitizer. Above 200–300 Hz we only observe distinct spectral peaks above the noise floor.

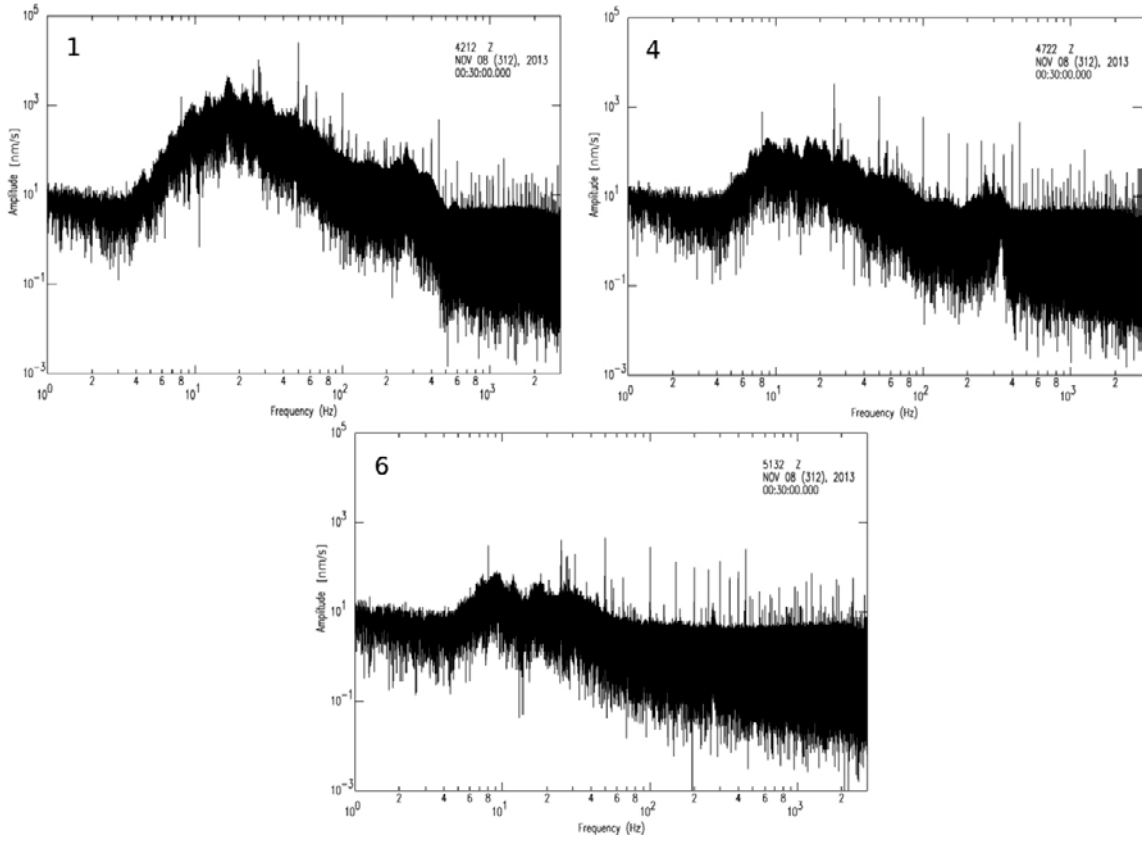

Figure 4-1. *Spectra of 10 minutes of data from 00:30 GMT on 2013-11-08. Data recorded at sites 1, 4 and 6 as indicated in the spectra. Frequency in Hz and amplitude in nm/s.*

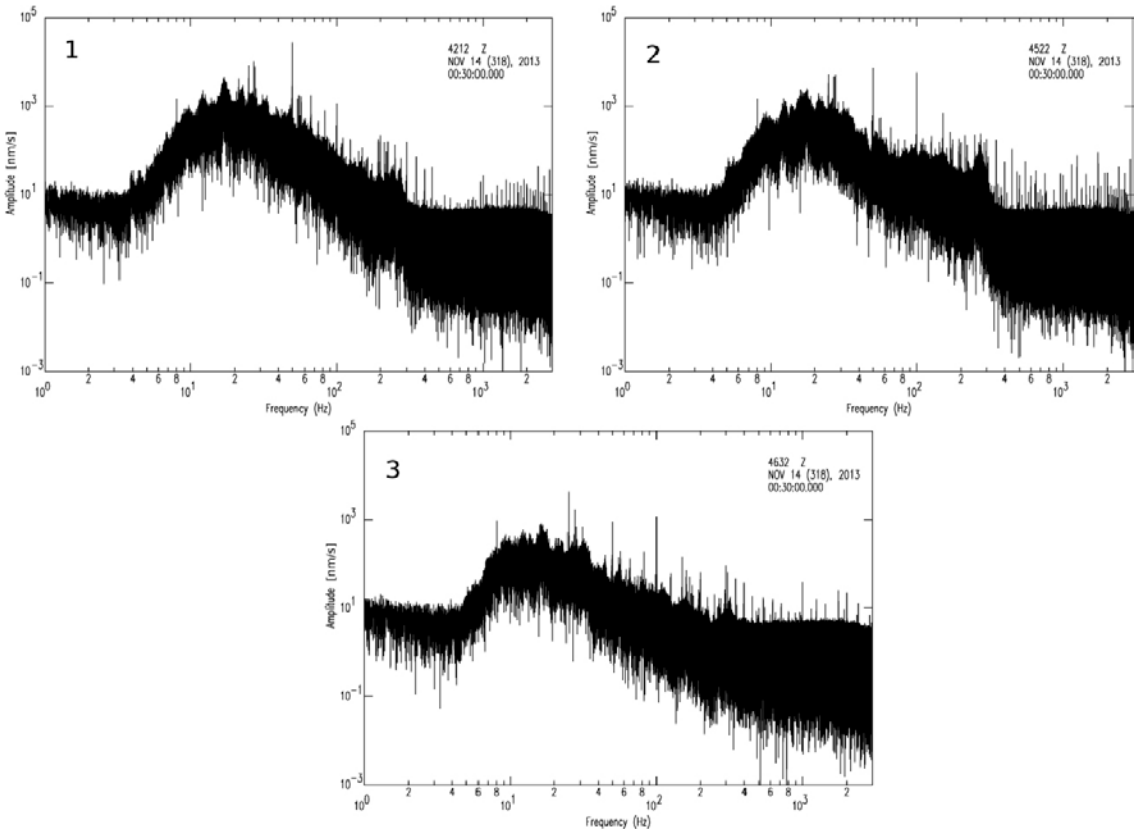

Figure 4-2. *Spectra of 10 minutes of data from 00:30 GMT on 2013-11-14. Data recorded at sites 1, 2 and 3 as indicated in the spectra. Frequency in Hz and amplitude in nm/s.*

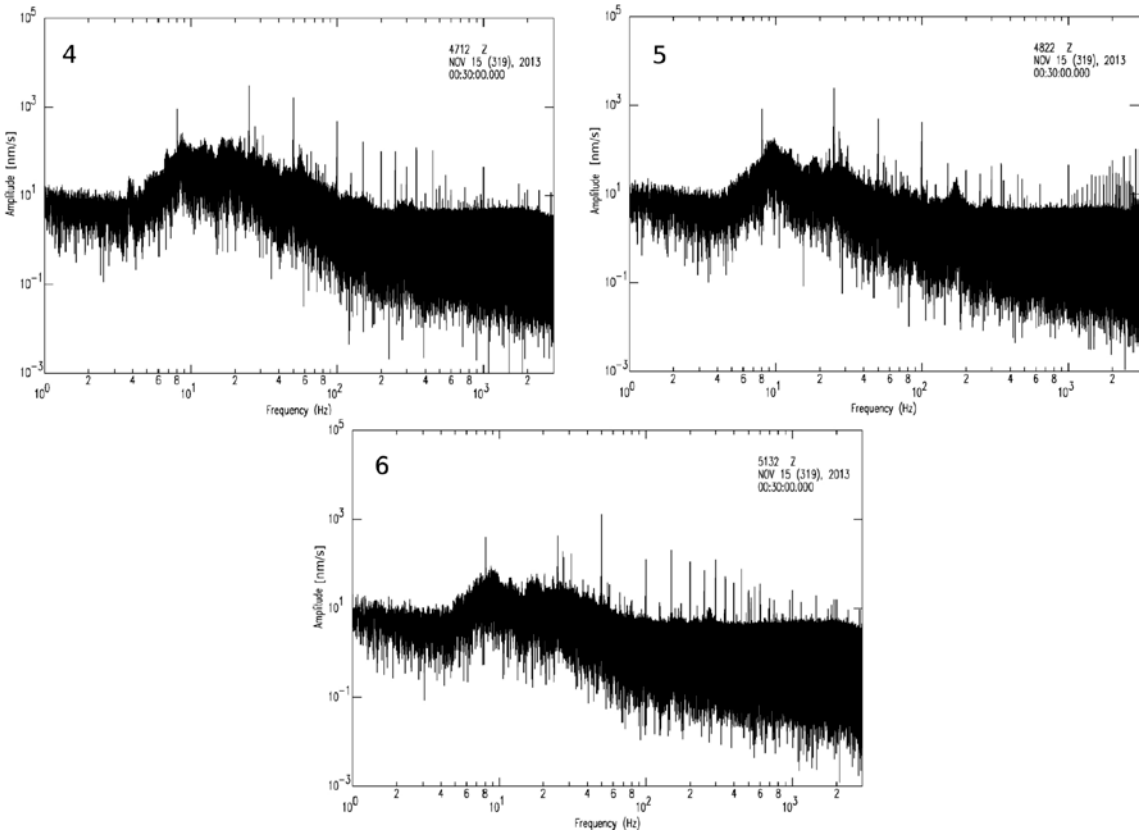

Figure 4-3. *Spectra of 10 minutes of data from 00:30 GMT on 2013-11-15. Data recorded at sites 4, 5 and 6 as indicated in the spectra. Frequency in Hz and amplitude in nm/s.*

The spectral “humps” observed at varying frequencies between approximately 150–300 Hz in Figures 4-1 to 4-3 are of unknown origin. Studying large numbers of spectra we find that the humps are not specific to certain sensors or sensor/digitizer combinations, so they are not internal to the instruments. In addition, they are not specific to specific sites or boreholes, as they vary in amplitude and frequency at the same site when different instruments are used. We interpret these humps as originating from insufficient coupling of the instruments to the boreholes, resulting in vibrations, resonances and/or standing waves in the boreholes. During the initial tests these humps were more pronounced but they decreased as we added the 2 kg lead weights to the sensor assemblies. The humps are unfortunate as they occur in the spectrum where the signal to noise ratio is decreasing, making it difficult to infer just where the electronic noise meets the ground motion.

The amplitude of the spectral peaks generally decay away from the nuclear power plants. For the discussion here it is important to note that as of this writing we do not have any information from the Forsmark nuclear power plants on where these signals may be generated. In Figure 4-4 we show four characteristic spectral peaks in the data. Note, however, that the data from sites 1, 2 and 3 are recorded 24 hours prior to the data at sites 4, 5 and 6, which implies that the source strength may differ between the two data sets. There is a very distinct peak at 8.04 Hz, which has similar amplitude at sites 1 and 2 indicating an origin in the power plants. As site 1 is 410 m away from Forsmark 2 and site 2 is 460 m away from Forsmark 1, the very similar amplitudes may point to similar sources in the two plants. We note that on the second day (sites 4, 5 and 6) the spectral peak is shifted to slightly lower frequencies and the background noise signals seem slightly lower than on the day before.

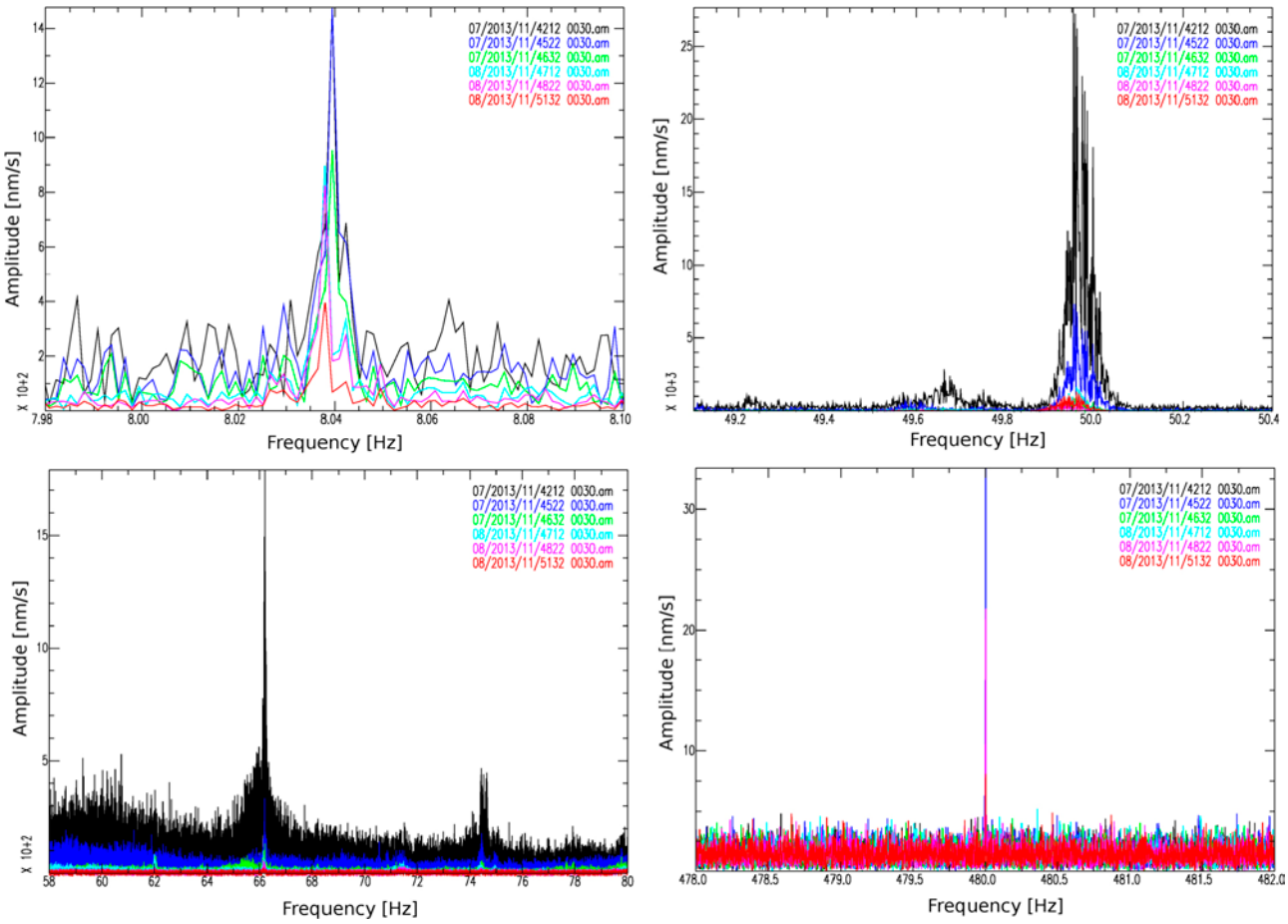

Figure 4-4. *Spectral peaks at frequencies 8 Hz (upper left), 50 Hz (upper right), 66 and 74 Hz (lower left) and 480 Hz (lower right). The colours indicate different sites: 1 black, 2 blue, 3 green, 4 cyan, 5 magenta, 6 red. Data at sites 1, 2 and 3 are recorded on 2013-11-14, at sites 4, 5 and 6 on 2013-11-15.*

The 50 Hz signal shows that the sensors pick up energy in a frequency band from approximately 49.9 to 50.1 Hz, and that there is an additional small hump at approximately 49.6–49.7 Hz. The 50 Hz signal is significantly stronger at site 1 than at site 2, which indicates a source closer to site 1 than site 2. We also see that the amplitudes decay away from the power plants. The data for the 66 Hz and 74 Hz signals show a similar pattern to the 50 Hz signal, with significantly higher amplitudes at site 1 and a decay in amplitude with distance from the power plants. The 480 Hz signal in Figure 4-4 is very narrow-band and does not decay away from the power plants. It is, as discussed above, the internal ethernet communication in the data logger that produces this signal. Shielding of cables and proper grounding will reduce the 480 Hz and over tones signal, as discussed with IMS (D. Bredenkamp, personal communication, 2014-02-12). In Table 4-1 we list the more pronounced spectral peaks in the data.

Probable external spectral peaks

Frequency [Hz]	Comment
8.04	Very strong at all sites
10–60	Wide hump
No 16.6	No signal from the railroad
24.8 (smaller) and 25	High amplitude at all sites
27.02, 27.51, 28.02 and 28.35	
50 (49.95)	Largest signal in the area, visible over-tones every 50 Hz to 950 Hz
54, 55, 56.7	
66.2, 74.5	
82.6	
124, 125	
175, 193, 194	
213.2, 224	

Probable internal spectral peaks

Frequency [Hz]	Comment
480, 640, 720, 760, 960, 1 440, 1 920	Internal ethernet communication
768, 864, 1 000, 1 056, 1 152, 1 344, 1 536, 1 632, 1 728, 1 824, 2 000	Very narrow band
1 150, 1 250, 1 350, 1 450, 1 750	

5 Spatial and temporal amplitude variations

We can investigate the temporal and spatial stability of the background seismic wave field during the three time periods when we recorded at different stations along the profile. The recordings took place from afternoon to morning on the 7–8, 13–14 and 14–15 of November, 2013. On the 7–8 we recorded at sites 1, 4 and 6, on the 13–14 at sites 1, 2 and 3 and on the 14–15 at sites 4, 5 and 6. The geophone data were bandpass filtered in the frequency intervals 10–30 Hz, 47–53 Hz and 105–120 Hz and we calculate the root mean square (rms) amplitude in 1 minute intervals. The resulting rms time series are shown in Figures 5-1 to 5-3.

In general, the signals behave as expected, assuming that the source of much of the wave field emanate from the nuclear power plants. In the 10–30 Hz band, A in the figures, the amplitudes decrease away from the power plants, and the amplitudes are similar at particular stations during different time periods. We note though that at site 6, the data contain more spikes than at other distances, only some of which correlate with spikes at the other stations. In the 50 Hz band, B in the figures, there is also a general decrease in amplitude away from the power plants, but we see that the amplitudes vary at a certain station on different days, and that on the 14–15th the amplitudes at site 6 are actually higher than those at site 5, it's neighbor toward the plants. Interestingly, the signals at site 6 on this day, the 14–15th, have higher amplitudes than those at site 6 on the 7–8th, whereas the signals at site 5 on the 14–15th have amplitudes more similar to those at site 6 on the 7–8th. The reason for this is unclear to us.

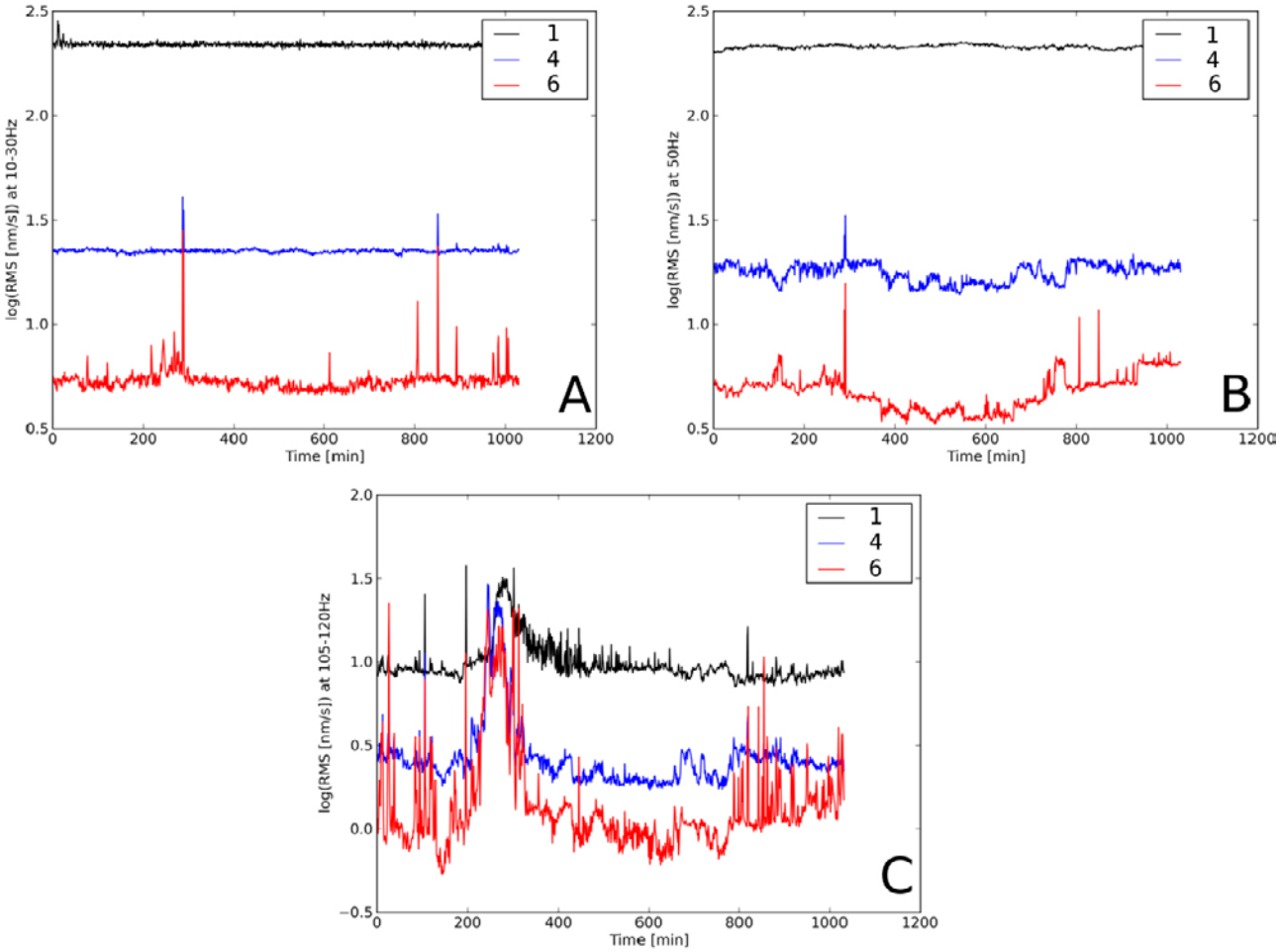

Figure 5-1. *Temporal geophone amplitude variations in three different frequency bands at sites 1 (black), 4 (blue) and 6 (red) on the 7–8 November, 2013. A) 10–30 Hz band. B) 47–53 Hz band. C) 105–120 Hz band. Time in minutes from 16:50 GMT, amplitudes as the logarithm of 1 minute interval root mean square values.*

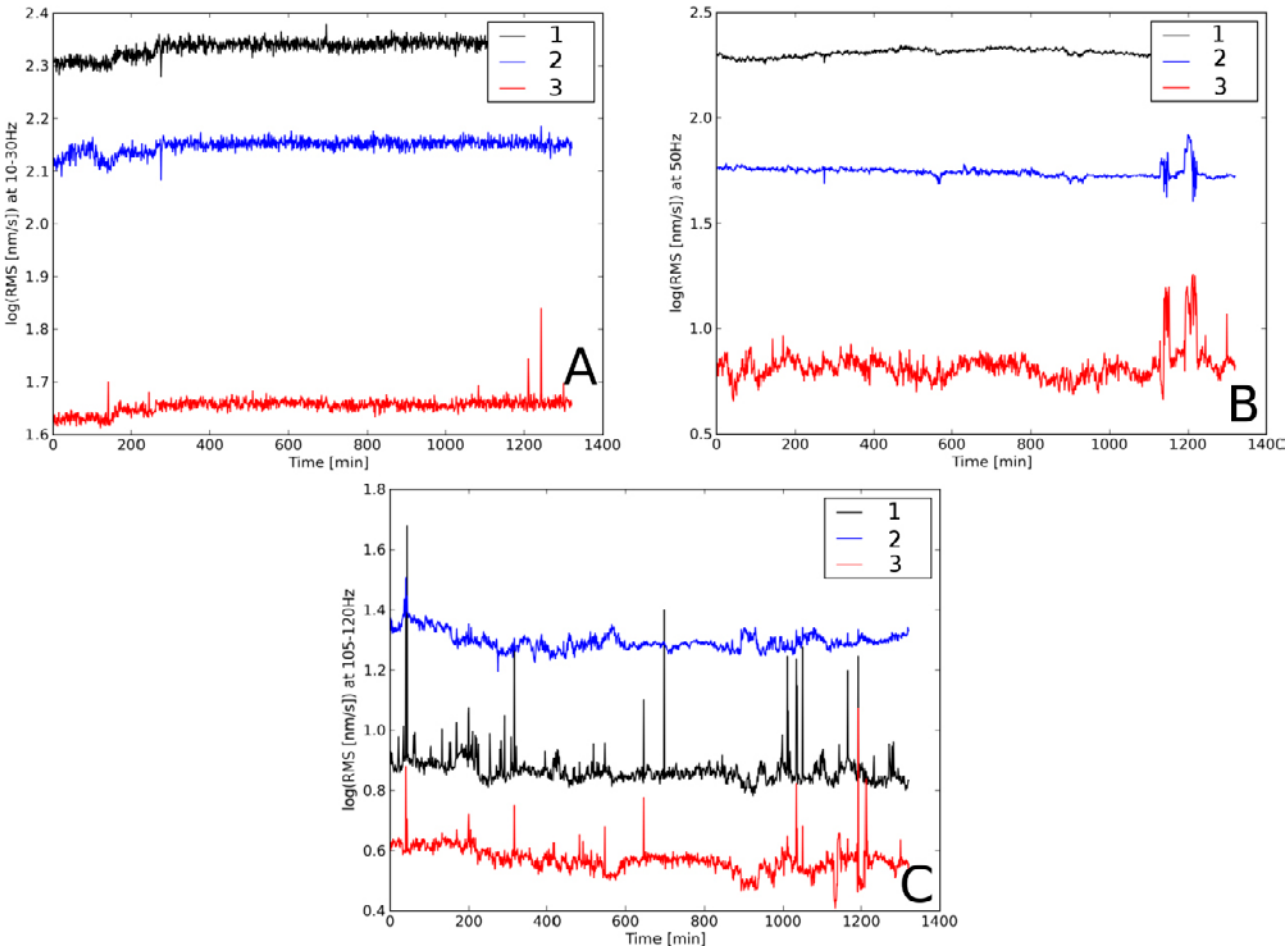

Figure 5-2. *Temporal geophone amplitude variations in three different frequency bands at sites 1 (black), 2 (blue) and 3 (red) on the 13–14 November, 2013. A) 10–30 Hz band. B) 47–53 Hz band. C) 105–120 Hz band. Time in minutes from 13:30 GMT, amplitudes as tlogarithm of 1 minute interval root mean square values.*

In Figure 5-4 we show a short segment of the actual waveform data for 15 November, filtered between 40 and 60 Hz, and we see that site 6 has indeed larger amplitudes than site 5. Importantly, Figure 5-4 shows that the signals are not in phase, indicating that the signal is in fact seismic and not electromagnetic.

In the 105–120 Hz band, C in the figures, there is much more temporal variation in the signal amplitudes, both in terms of short term spikes and longer term variations. Although two recording days show the expected amplitude decay away from the power plants, the recordings from the closer three stations, Figure 5-2, show higher amplitudes at station 2 than at station 1. Both of these stations are at similar distances to two different reactors, so we speculate that the 105–120 Hz signal either originates in the vicinity of the power plant closest to site 2, or that during this day the signal was stronger from that plant.

Investigating the spatial and temporal variation in accelerometer amplitudes in two frequency bands, 4–6 kHz and 8–10 kHz, the resulting rms time series are shown in Figure 5-5 and 5-6. We see that the amplitudes are very stable, and that they vary very little through a measurement day. We also note that they do not vary significantly from site to site. This probably implies that we observe mostly internal electronic noise, and that there seems to be no high-frequency generating source in the vicinity of the measurement sites.

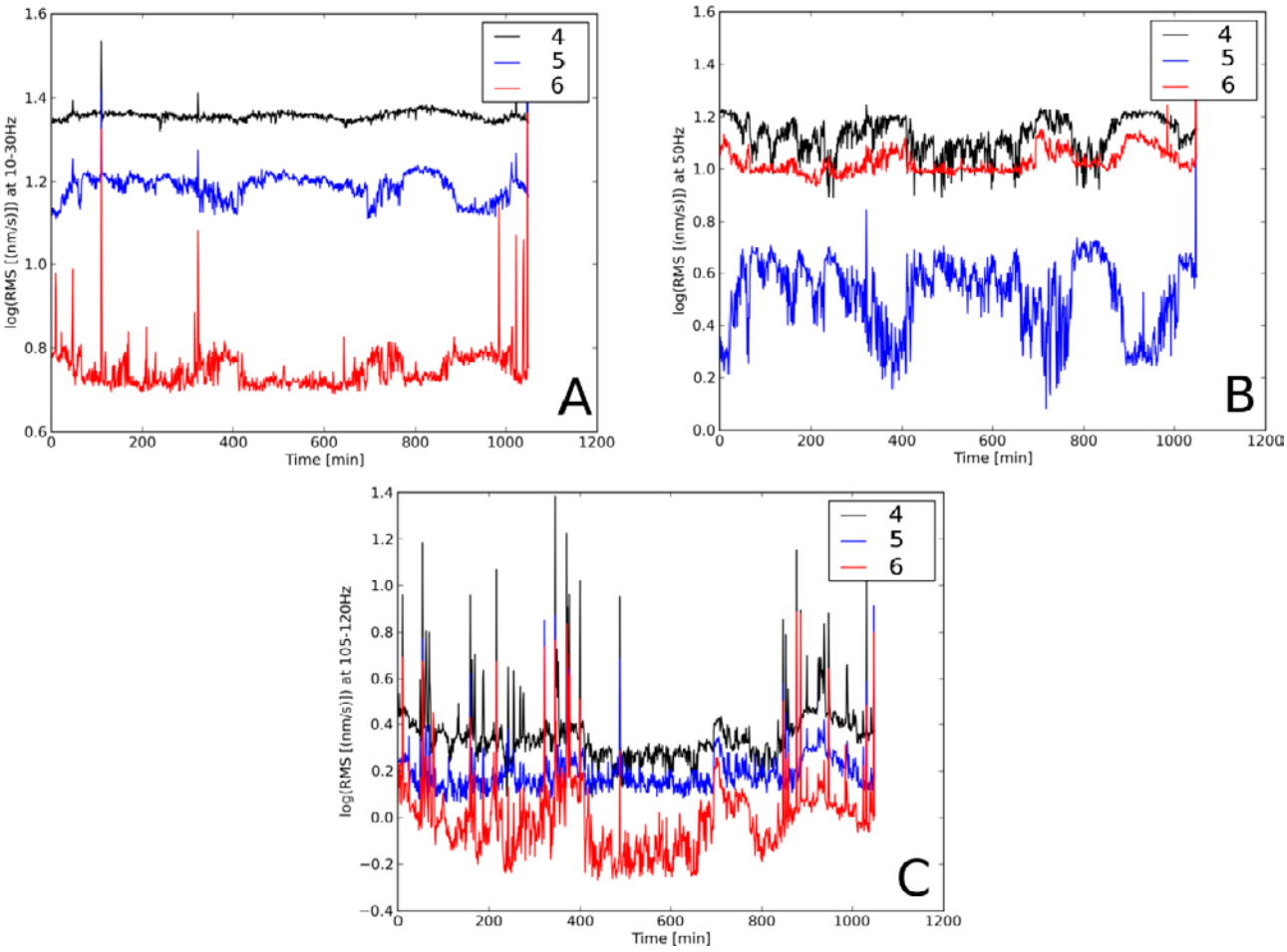

Figure 5-3. *Temporal geophone amplitude variations in three different frequency bands at sites 4 (black), 5 (blue) and 6 (red) on the 14–15 November, 2013. A) 10–30 Hz band. B) 47–53 Hz band. C) 105–120 Hz band. Time in minutes from 16:10 GMT, amplitudes as the logarithm of 1 minute interval root mean square values.*

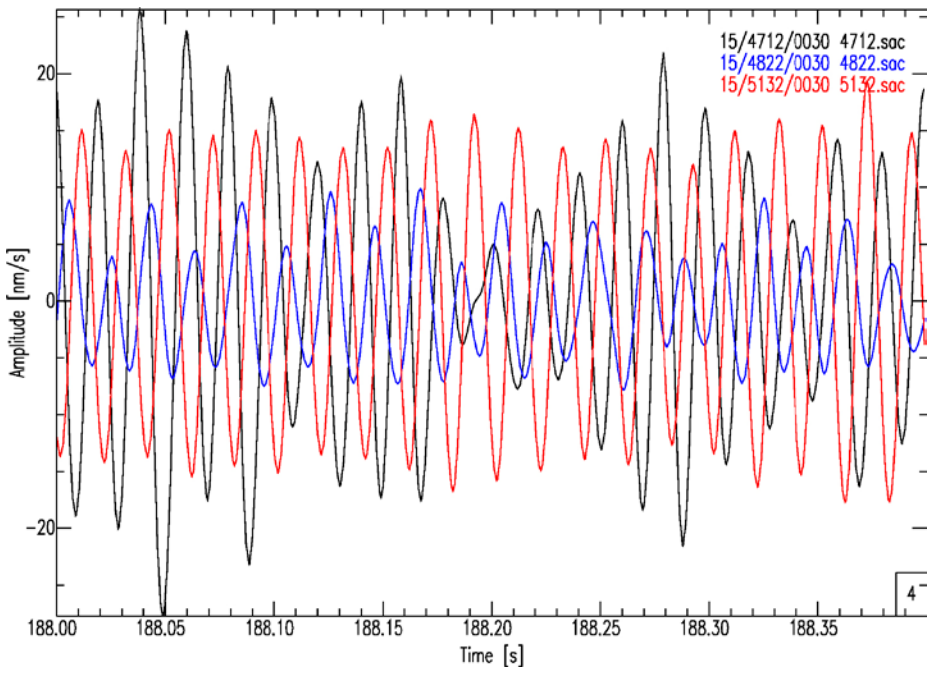

Figure 5-4. *Temporal geophone amplitude variations in the frequency band 40–60 Hz at sites 4 (black), 5 (blue) and 6 (red) on the 14 November, 2013. Time in seconds from 00:30 GMT, amplitude in nm/s.*

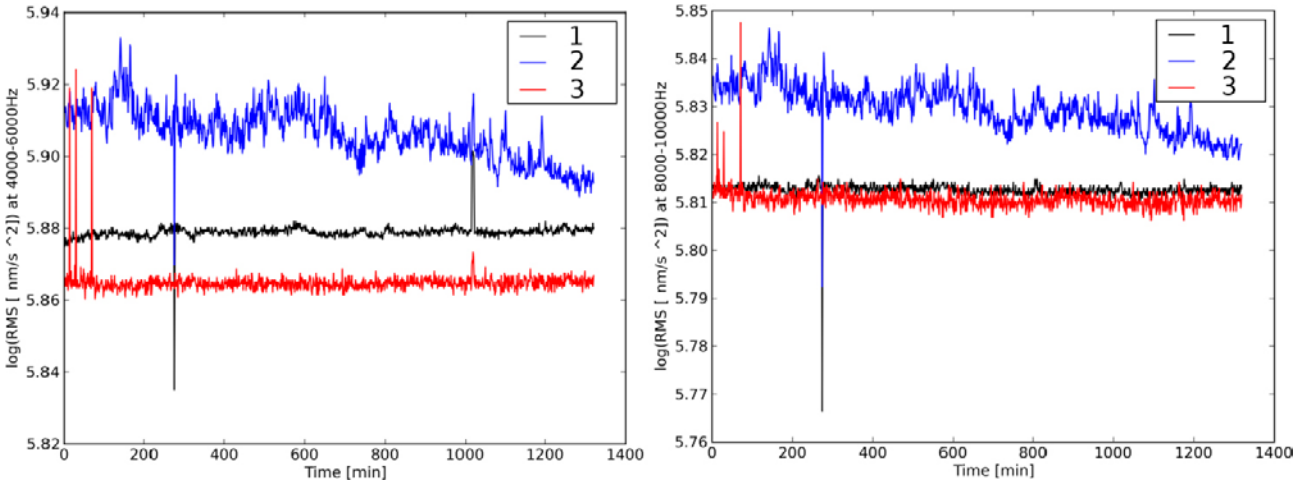

Figure 5-5. *Temporal accelerometer amplitude variations in two different frequency bands at sites 1 (black), 2 (blue) and 3 (red) on the 13–14 November, 2013. Left) 4–6 kHz band. Right) 8–10 kHz band. Time in minutes from 13:30 GMT, amplitudes as the logarithm of 1 minute interval root mean square values.*

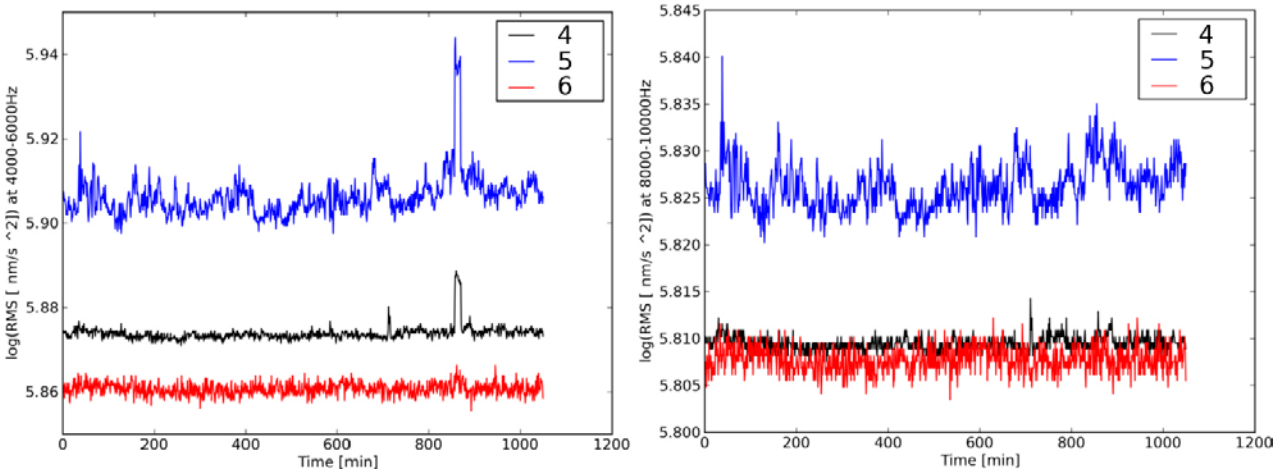

Figure 5-6. *Temporal accelerometer amplitude variations in two different frequency bands at sites 4 (black), 5 (blue) and 6 (red) on the 14–15 November, 2013. Left) 4–6 kHz band. Right) 8–10 kHz band. Time in minutes from 16:10 GMT, amplitudes as the logarithm of 1 minute interval root mean square values.*

6 Correlation analysis for instrument performance

An efficient approach to evaluate how well instruments can resolve true ground motion is to record the seismic background signals using multiple instruments located close together (e.g. Wielandt 2002, Sleeman et al. 2006). The instruments will record common signals, and if the instruments are sensitive enough, these signals will correlate very well. The Swedish National Seismic Network has used this methodology to test all new incoming instruments over the last 15 years. Data is recorded over night, a quiet 10 minute period during the night is selected as test data and the correlation over a range of frequency bands is calculated. At Forsmark, all three IMS sensors recorded simultaneously, using the same data logger, over night at sites 1 and 6. The resulting geophone spectra are shown in Figures 6-1 and 6-2.

The spectra show that some frequency bands look very similar between sensors, but that in other frequency bands there are significant variations, such as the variation in the location of the hump discussed above.

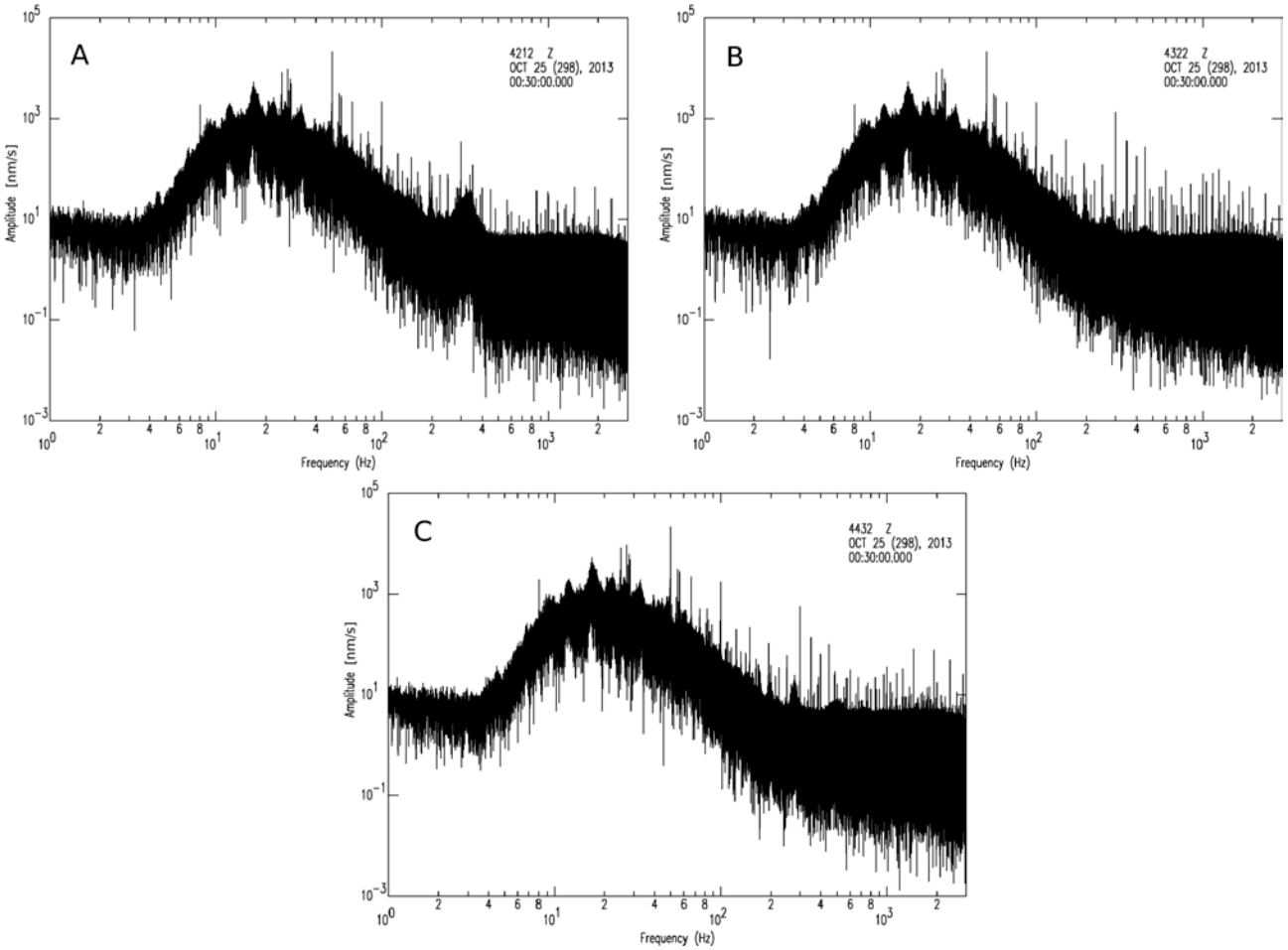

Figure 6-1. *Geophone spectra from site 1 on 25 October, 2013 at 00:30 GMT. 10 minutes of data sampled at 6 kHz. Sensors 1, 2 and 3 in A, B and C, respectively.*

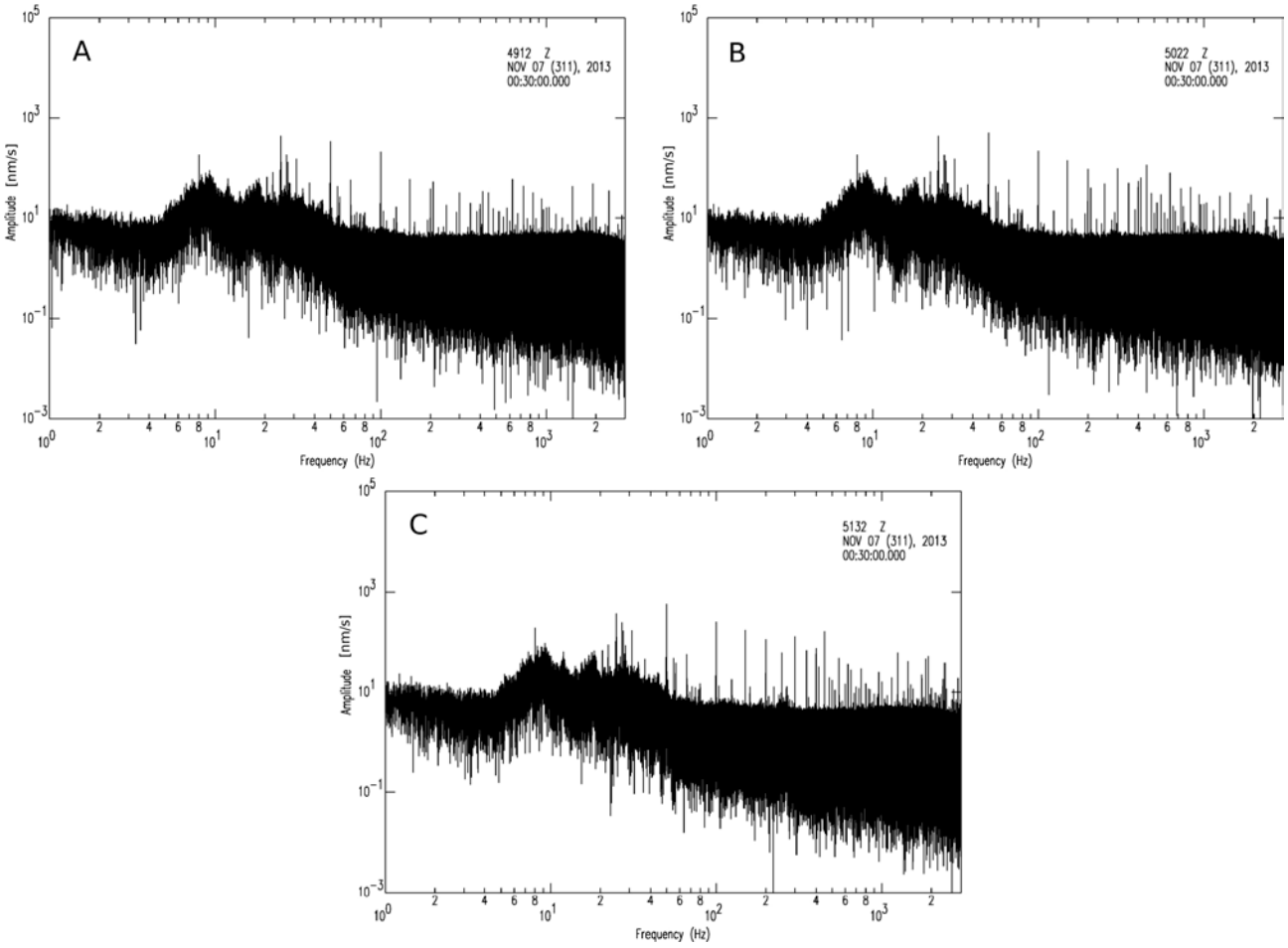

Figure 6-2. *Geophone spectra from site 6 on 7 November, 2013 at 00:30 GMT. 10 minutes of data sampled at 6 kHz. Sensors 1, 2 and 3 in A, B and C, respectively.*

Correlation in the frequency domain quantifies the similarities in the spectra and Figure 6-3 shows the geophone correlation curves. We see, as expected, that the recorded amplitudes are significantly lower at site 6 than at site 1. Lower amplitude signals usually mean poorer correlation as uncorrelated noise from the instrumentation has a larger impact. This is also clear from the correlation curves in Figure 6-3, we see that at site 1 the instruments correlate well (above 0.9) from approximately 4 Hz to 150 Hz, while at site 6 the correlation coefficient never reaches 1, and the well correlating interval extends from approximately 5 Hz to 80 Hz. We note that the spectral "humps" observed at frequencies between 150 Hz and 300 Hz and discussed above, probably are partly responsible for degrading the correlation above 100–150 Hz.

The correlation results obtained here indicate that the IMS instrument configurations are not able to observe quiet background ground motions outside of the 5–100 Hz interval, approximately, in spite of the good digitizer specifications. A larger interval could be obtained by either adding a low noise pre-amplifier to the sensors, or adding more sensor elements to the geophone assembly. The latter will however see an increase in the effect of the current noise from the assembly.

The gain in the length of the well correlating frequency interval can be estimated by comparing the results with the custom made five-element geophones used in this study to regular one-element geophones. We showed in Section 2.2 that the sensitivity of the five-element geophone assembly is 250 V/m/s, a gain with a factor 4.2 compared to the 60 V/m/s sensitivity of the one-element geophone. If we use this factor to decrease the spectral amplitudes measured with the geophone assembly in the field, we can simulate a one-element geophone and directly see how much resolution is lost with respect to the internal noise levels in the digitizer. Figure 6-4 shows how this reduction in

amplitude would affect the data from sites 1 and 6 and it is clear that with a one-element geophone at the quiet site 6, we would not have been able to record more than a few spectral peaks above the digitizer noise. Figure 6-4 nicely illustrates the advantage of using a multiple geophone assembly to increase the sensitivity of the sensor, and thereby allow the recording, and detection, of weaker signals without installation of more sensors.

A correlation analysis on the accelerometer data was attempted but failed due to the noisy accelerometer system, as was evident already from Figure 3-3.

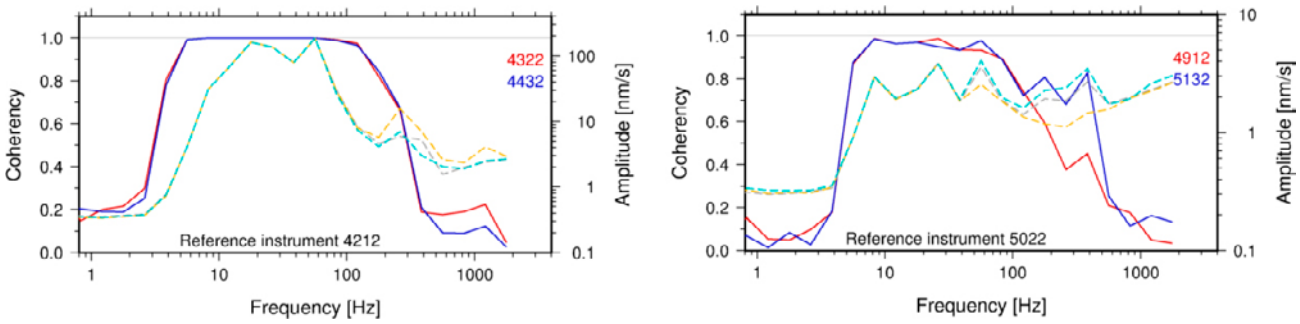

Figure 6-3. *Correlation and amplitude curves for three IMS instruments recording at site 1 (left) and site 6 (right). 10 minutes of data at 00:30 GMT on 25 October and 7 November, respectively. Two correlation curves (red, blue, as the sensor IDs) for each site with the reference sensor ID noted in black, scale to the left. Three amplitude curves, scale to the right in nm/s, reference sensor (grey) and the two test sensors with orange corresponding to the red sensor, and cyan to the blue sensor.*

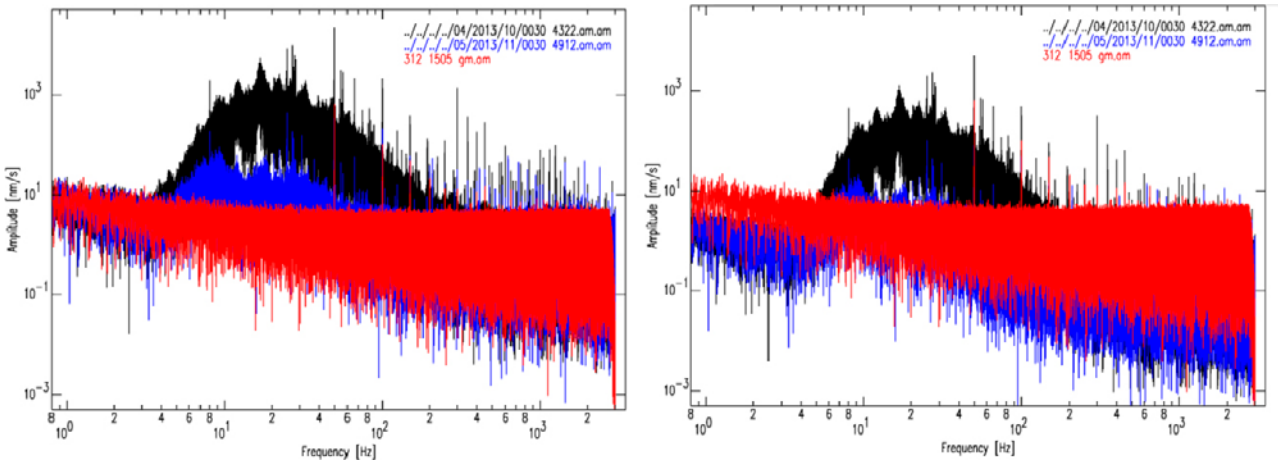

Figure 6-4. *Spectra with 10 minutes of data from site 1 (black) on 25 October 2013 at 00:30 GMT, site 6 (blue) on 7 November 2013 at 00:30 GMT, and from the laboratory measurements on the logger (red), see Section 2.2. Left) Using the sensor sensitivity of the five element geophone assembly. Right) Simulated sensor with a single-geophone element.*

7 Recommendations for the design of a seismic network at Forsmark

One of the main results of this study is the realization that with geophones with too low sensitivity (corresponding to normal single geophone sensitivity), we will not be able to record true ground motion in the frequency band of interest for the repository seismic network. The study shows that geophones with nominal sensititvity of at least 400 V/m/s, given the noise characteristics of the IMS digitizer, should be used to be able to record true ground motion over the entire repository area. An additional, external high-quality pre-amlifier would also increase the sensitivity. Borehole geophones should be used, and once these are thoroughly coupled to the bedrock, e.g. by cementing, the response will most likely improve, in certain frequency bands, compared to the results obtained in this study.

There is significant seismic noise from the nuclear power plants in the repository region, both wide-band noise below 100 Hz and narrow-band high-noise levels at higher frequencies. This will be a challenge for the repository seismic network. We suggest that the network initially is instrumented with a limited number of high-sensitivity geophones, ideally placed in boreholes at 30–200 m depth, below the gently dipping fracture zone that covers much of the repository area. The borehole stations should be augmented by a few surface stations, especially in the vicinity of the construction of the tunnel. As excavations progress and seismic events from the construction are being analyzed, the network should be gradually expanded based on the need to improve the analysis and to cover certain volumes more accurately. If smaller seismically active volumes are identified at depth, then there may be a need for a dense installation of geophones or accelerometers in that volume. The repository network should also be linked to the Swedish National Seismic Network (SNSN) in order to improve the analysis of larger events.

As a next step toward the realization of the network, we suggest a detailed network design phase where this and the previous seismic noise study (Lund et al. 2012) are combined with information on available boreholes, suitable sites for surface installations and the repository layout. In addition, a thorough inventory of commercially available hardware, software and support should be performed to aid the design decisions. Issues such as time syncronization, downhole digitizers and data communication should be analyzed. Experience from running local, high resolution networks should be gathered from e.g. the Finnish repository network at Olkiluoto and the LKAB mines in Kiruna and Malmberget.

References

SKB's (Svensk Kärnbränslehantering AB) publications can be found at www.skb.com/publications.

Lund B, Bödvarsson R, Shomali H, Dynesius L, 2012. Forsmark site investigation. Study of seismic background signals in the Forsmark area. SKB P-12-08, Svensk Kärnbränslehantering AB.

SACLAB, 2014. Software downloads. Available at: http://web.utah.edu/thorne/software.html [29 March 2017].

Sleeman R, van Wettum A, Trampert J, 2006. Three-channel correlation analysis: a new technique to measure instrumental noise of digitizers and seismic sensors. Bulletin of the Seismological Society of America 96, 258–271.

Wielandt E, 2002. Seismic sensors and their calibration. In Bormann P (ed). IASPEI New manual of seismological observatory practice. Vol 1. GeoForschungsZentrum Potsdam, Germany.

Sensor Specification – Uppsala Special Build

Sensor Specification

Uppsala Special Build

Document Number
SKB-SPEC-201309-EdK rev 0

Accelerometer Element		
Description	**Value**	**Tolerance**
Type	25 kHz	-
Configuration	Uniaxial, Vertical	-
Sensitivity	100 mV/g	±5%
Broadband Noise	150 μg	-
Geophone Element		
Description	**Value**	**Tolerance**
Type	Omni directional	-
Natural Frequency	14 Hz	±7%
Configuration	Uniaxial, Vertical	-
Open Circuit Damping	0.185	+10/-5%
Coil Resistance	3500 Ω	±5%
Open Circuit Sensitivity	80 V/m/s	+5/-10%
RtBcFn	49931 Ω Hz	-
Moving Mass	10.2 g	-

Assembled Configuration	
Geophone	5 elements, series, vertical
Accelerometer	1 element, vertical
Geophone Assembly	
Open Circuit Damping	0.185
Coil Resistance	17500 Ω
Open Circuit Sensitivity	400 V/m/s
RtBcFn	249655 Ω Hz
Nominal damping resistor	41 kΩ
Damping ratio with above	0.49
Sensor Cable	
Signal	**Colour**
Geophone (+)	Red
Geophone (-)	Blue
Not Used	Yellow
Not Used	Green
Accelerometer (+)	White
Accelerometer (-)	Black
Not Used	Brown
Not Used	Purple

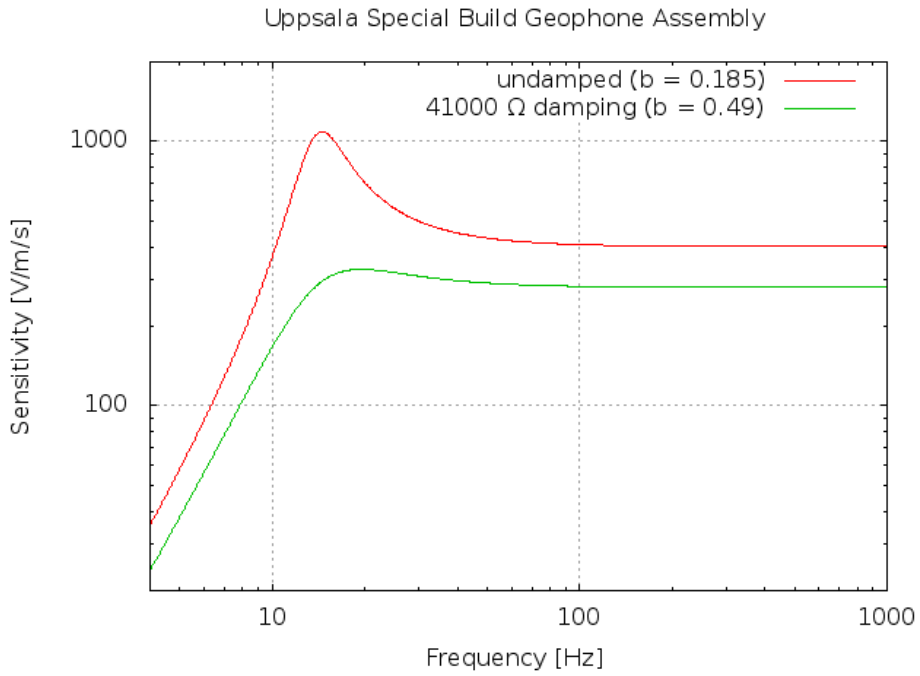

Characteristics of IMS 14 Hz geophones

Characteristics of IMS 14 Hz geophones

Sensor

Working position:	Omni-directional
Frequency range	9 Hz to >2000 Hz
Natural frequency	14 Hz ± 7%
Distortion with 18 mm/s p.p. coil to case velocity	< 0.7%
Distortion measurement frequency	14 Hz
Open circuit damping	0.185 ± 10%
Standard coil resistance	3500 Ohm ± 5%
Open circuit sensitivity	80 V/m/s ± 10%
Damped (0.7) sensitivity	60 V/m/s ± 10%
Moving mass	10g
Maximum coil excursion p.p.	0.5 mm

Physical

diameter	51 mm
length	230 mm
mass	1.5 kg

November 2011

ISO9001 document number: ISSREP-017-v1

Arkitektkopia AB, Bromma, 2017

SKB is tasked with managing Swedish nuclear and radioactive waste in a safe way.

skb.se